Cancer Letters 445 (2019) 24–33

Contents lists available at ScienceDirect

Cancer Letters

journal homepage: www.elsevier.com/locate/canlet

Original Articles

Synergistic activity of BET inhibitor MK-8628 and PLK inhibitor Volasertib in preclinical models of medulloblastoma

Youjia Han[a], Sven Lindner[b], Yi Bei[a], Heathcliff Dorado Garcia[a], Natalie Timme[a], Kristina Althoff[b], Andrea Odersky[b], Alexander Schramm[b], Andrej Lissat[a], Annette Künkele[a,c,d], Hedwig E. Deubzer[a,c,d,e], Angelika Eggert[a,c], Johannes H. Schulte[a,c], Anton G. Henssen[a,c,d,*]

[a] Department of Pediatric Oncology/Hematology, Charité-Universitätsmedizin Berlin, Germany
[b] Department of Pediatric Oncology and Hematology, University Children's Hospital Essen, Essen, Germany
[c] German Consortium for Translational Cancer Research (DKTK), Berlin, Germany
[d] Berlin Institute of Health (BIH), Berlin, Germany
[e] Experimental and Clinical Research Center (ECRC) of the Charité and the Max-Delbrück-Center for Molecular Medicine (MDC) in the Helmholtz Association, Berlin, Germany

ARTICLE INFO

Keywords:
BRD4
MYC
PLK1
Pediatric brain tumors
Targeted therapy

ABSTRACT

Medulloblastoma is the most prevalent central nervous system tumor in children. Targeted treatment approaches for patients with high-risk medulloblastoma are needed as current treatment regimens are not curative in many cases and cause significant therapy-related morbidity. Medulloblastoma harboring *MYC* amplification have the most aggressive clinical course and worst outcome. Targeting the BET protein BRD4 has significant anti-tumor effects in preclinical models of *MYC*-amplified medulloblastoma, however, in most cases these are not curative. We here assessed the therapeutic efficacy of the orally bioavailable BRD4 inhibitor, MK-8628, in preclinical models of medulloblastoma. MK-8628 showed therapeutic efficacy against *in vitro* and *in vivo* models of *MYC*-amplified medulloblastoma by inducing apoptotic cell death and cell cycle arrest. Gene expression analysis of cells treated with MK-8628 showed that anti-tumor effects were accompanied by significant repression of *MYC* transcription as well as disruption of MYC-regulated transcriptional programs. Additionally, we found that targeting of MYC protein stability through pharmacological PLK1 inhibition showed synergistic anti-medulloblastoma effects when combined with MK-8628 treatment. Thus, MK-8628 is effective against preclinical high-risk medulloblastoma models and its effects can be enhanced through simultaneous targeting of PLK1.

1. Introduction

Medulloblastoma is the most common malignant brain tumor in children. It arises from cerebellar cells and can be subdivided in four distinct clinical, biological and genetic subgroups, *i.e.* the Wingless (WNT), Sonic Hedgehog (SHH), group 3 and group 4 [1–3]. Group 3 tumors are characterized by the highest *MYC* expression and coincidental genomic *MYC* amplification [1–3]. Patients with group 3 medulloblastoma with high *MYC* expression have the worst clinical outcome with 5-year survival rates below 50% [4–6]. Due to the lack of novel targeted therapies, treatment of patients with group 3 medulloblastoma has not significantly improved over the past decade [1,4,6]. Therefore, new drugs are urgently needed for patients with group 3 medulloblastoma. As *MYC* is the central oncogenic driver of these tumors and tumors are highly dependent on *MYC* expression, *MYC* is an ideal drug target in group 3 medulloblastoma.

Maintenance of high *MYC* expression in cancer through transcriptional and post-translational modes has been extensively studied in the past years. For example, high abundance of certain histone modifications and concomitant recruitment of their epigenetic readers play an important role in the aberrant expression of oncogenes such as *MYC* [7,8]. Targeted inhibition of epigenetic readers recruited to *MYC* enhancers has opened new possibilities to influence the transcriptional regulation of *MYC* in cancer [9]. One prototypical example for this is the targeted inhibition of bromodomain and extra-terminal domain (BET) containing protein BRD4, which leads to repression of *MYC* transcription [10]. Bromodomain protein BRD4 binds to acetylated lysines in the N-terminal regions of histones and recruits transcriptional co-activators to H3K27 at enhancer sites [11,12]. Blocking the interaction of BRD4 with the H3K27Ac leads to downregulation of *MYC* and

* Corresponding author. Department of Pediatric Oncology/Hematology, Charité-Universitätsmedizin Berlin, Germany.
E-mail address: Henssenlab@gmail.com (A.G. Henssen).

https://doi.org/10.1016/j.canlet.2018.12.012
Received 2 October 2018; Received in revised form 5 December 2018; Accepted 11 December 2018

MYC target genes in various cancer entities [13–20]. In medulloblastoma, pharmacological BET inhibition is most potent in MYC-driven medulloblastoma models and one report has indicated specific inhibition of the hedgehog pathway in SHH-medulloblastoma [16,17,21,22]. MK-8628 is a selective small molecule BET protein inhibitor and has several advantages over previously described BRD4 inhibitors such as good oral bioavailability and favorable pharmacological properties in humans [20,23–27]. Future clinical introduction of this compound depends on in depth analysis of its efficacy in preclinical models.

Although BRD4 inhibition has promising efficacy against solid tumors, single agent treatment is not curative in preclinical *in vivo* models of medulloblastoma and will likely not cure patients when used alone [17,28]. We hypothesized that synergistic combination treatment approaches could increase efficacy to clinically relevant levels. Based on previous literature, we reasoned that one potential molecular target for such combination treatments could be Polo-like kinase 1 (PLK1) [29–31]. PLK1 is a serine/threonine kinase involved in the PDK1 pathway that binds directly to and phosphorylates MYC, stabilizing it in the late stage of cell cycle [32]. PLK1 is crucial for MYC regulation and for cancer cell survival due to its role in cell cycle regulation [30,32], and PLK1 inhibition can prevent proliferation, self-renewal, and cell-cycle progression of medulloblastoma cells and induces apoptosis [31]. Combination treatment with PLK1 inhibitors and BRD4 inhibitors has synergistic effects in leukemia, suggesting that this may also apply to other tumor entities such as medulloblastoma [33]. We here provide preclinical evidence that MK-8628 is similarly potent against MYC-driven medulloblastoma models as compared to previously described BET-inhibitors. Additionally, we show that combined BET and PLK1 inhibition exhibits synergistic anti-tumor activity in medulloblastoma. This may serve as a rationale for future clinical testing of BRD4 and PLK1 inhibitors in patients with high-risk medulloblastoma.

2. Materials and methods

2.1. Cell culture and in vitro treatment

The four human medulloblastoma cell lines were grown either in Dulbecco's Modified Eagle Medium (DMEM) (HD-MB3, UW228 and DAOY) or Roswell Park Memorial Institute medium (RPMI) 1640 (ONS-76), both supplemented with 10% FCS, L-glutamine, and 1% penicillin/streptomycin. The identity of all cell lines was verified by STR genotyping performed by the German Collection of Microorganisms and Cell Cultures (DSMZ, Braunschweig, Germany). Using PCR all cell lines were found to be free of mycoplasma (primers sequences available upon request). MK-8628-API (Active Pharmaceutical Ingredient) and Volasertib-API were purchased from Selleckchem (Munich, Germany) and GSK461364A was purchased from Axon Medchem (Groningen, Netherlands), aliquoted for single use and stored at −20 °C as a 10 mM stock solution in dimethyl sulfoxide (DMSO). For passaging and seeding, cell lines were washed with PBS, trypsinized and resuspended in fresh media, then counted using trypan blue dye staining. For treatment, cells were exposed to 0–10 μM MK-8628-API, 0–0.1 μM Volasertib-API, 0–0.3 μM GSK461364A-API or combinations of them prepared as serial dilutions in full medium. The final DMSO concentration was kept at or below 1%.

2.2. Cell proliferation, cell death, cell viability and cell cycle analysis

Medulloblastoma cell lines were seeded onto 96-well plates (500 cells per well) in triplicate for all assays, and incubated for 24h to permit surface adherence. Cells were treated with 0–10 μM MK-8628-AP, 0–0.1 μM Volasertib-API or combination of both. Viability was assessed 72h after treatment using the CellTiter-Glo Luminescent Cell Viability Assay (Promega, Wisconsin, USA) according to the manufacturer's protocol. The IC_{50} and area under the curve (AUC) were calculated using GraphPad Prism 7.0 (GraphPad Software Inc., San Diego, CA, USA) as previously described [34]. Apoptosis and proliferation were assessed after treatment with 500 nM MK-8628-API using the Cell Death and BrdU ELISA assays (Roche, Basel, Switzerland), respectively, after 24h, 48h and 72h of drug treatment. All assays were performed according to the manufacturer's protocols. For cell cycle analysis, cell lines were cultured for 72h in the presence of 500 nM MK-8628-API, 5 nM Volasertib-API, combination of both or DMSO control in 10 cm dishes at 3.5×10^5 cells/dish. Cells were harvested after 2h incubation with EdU, then DNA was stained with propidium iodide using Click-iT Plus™ EdU Flow Cytometry Assay Kits (Thermo Fisher Scientific, Massachusetts, USA) as described before [35]. Cellular DNA content was analyzed in a BD LSRFortessa X-20 (BD Biosciences, California, USA). All experiments were independently performed at least 3 times, if not otherwise indicated.

2.3. Quantitative reverse transcription polymerase chain reaction (qRT-PCR)

Total RNA was extracted from cells using RNeasyMini kit (Qiagen, Hilden, Germany) according to the manufacturer's protocol and concentration was determined with Nanodrop (Thermo Fisher Scientific). For *CCND1*, cDNA synthesis was performed using the SuperScript reverse transcription kit (Invitrogen, Darmstadt, Germany) and its expression was monitored using Assays-on-Demand™ (Applied Biosystems, Foster city, CA, USA). Expression values were normalized to the geometric mean of GAPDH [36]. Data analysis and error propagation were performed using the qbasePLUS software version 1.5 (http://www.biogazelle.com). For *MYC*, cDNA was synthesized using the Transcriptor First Strand cDNA Synthesis Kit (Roche) and its expression was measured using StepOne Plus™ (Applied Biosystems). Expression values were normalized to the geometric mean of HPRT1 as described before [36]. Data analysis and error propagation were performed using the (StepOne Software v2.3 (Applied Biosystems). All experiments were independently performed at least 3 times, if not otherwise indicated.

2.4. Western blot analysis

Protein lysates were extracted from cells, separated on NuPAGE 10% Bis-Tris Gel (Invitrogen) and electro-transferred on Polyvinylidene difluoride (PVDF) membranes (Roche). Membranes were incubated for 1h with 10% nonfat dry milk (or 5% BSA for phospho-antibodies) in tris-buffered saline plus 0.1% Tween 20 (TBS-T), then incubated with primary antibodies in 10% nonfat dry milk (or 5% BSA for phospho-antibodies) in TBS-T overnight at 4 °C. Primary antibodies against the following proteins and dilutions were used: MYC (1:500, #9402, Cell Signaling Technology (CST), Danvers, MA, USA), BRD4 (1:200, H-250, sc-48772, Santa Cruz, Dallas, TX, USA), WEE1 (1:1000, sc-5285, Santa Cruz), CCND1 (1:500, #2922, CST), E2F1 (1:200, AF4825, R&D Systems, Minneapolis, MI, USA), PLK1 (1:500, H-152, sc-5585, Santa Cruz), phospho-PLK1 (1:200, ab39068, Abcam, Cambridge, UK) and beta-actin (1:20000, 3700S, CST). After washing thrice with TBS-T, membranes were incubated 1h at room temperature with secondary antibodies diluted 1:5000 in 10% nonfat dry milk (or 5% BSA for phospho-antibodies) in TBS-T. Horseradish peroxidase (HRP)-conjugated anti-rabbit IgG (111-035-003, Dianova, Hamburg, Germany) or HRP-conjugated anti-mouse IgG (115-035-003, Dianova) were used as secondary antibodies. Proteins were visualized using the ImmunoCruz™ Western Blotting Luminol Reagent (Santa Cruz) and analyzed on a FusionFX7 detection device (Vilber Lourmat, Eberhardzell, Germany). All experiments were independently performed at least 3 times, if not otherwise indicated.

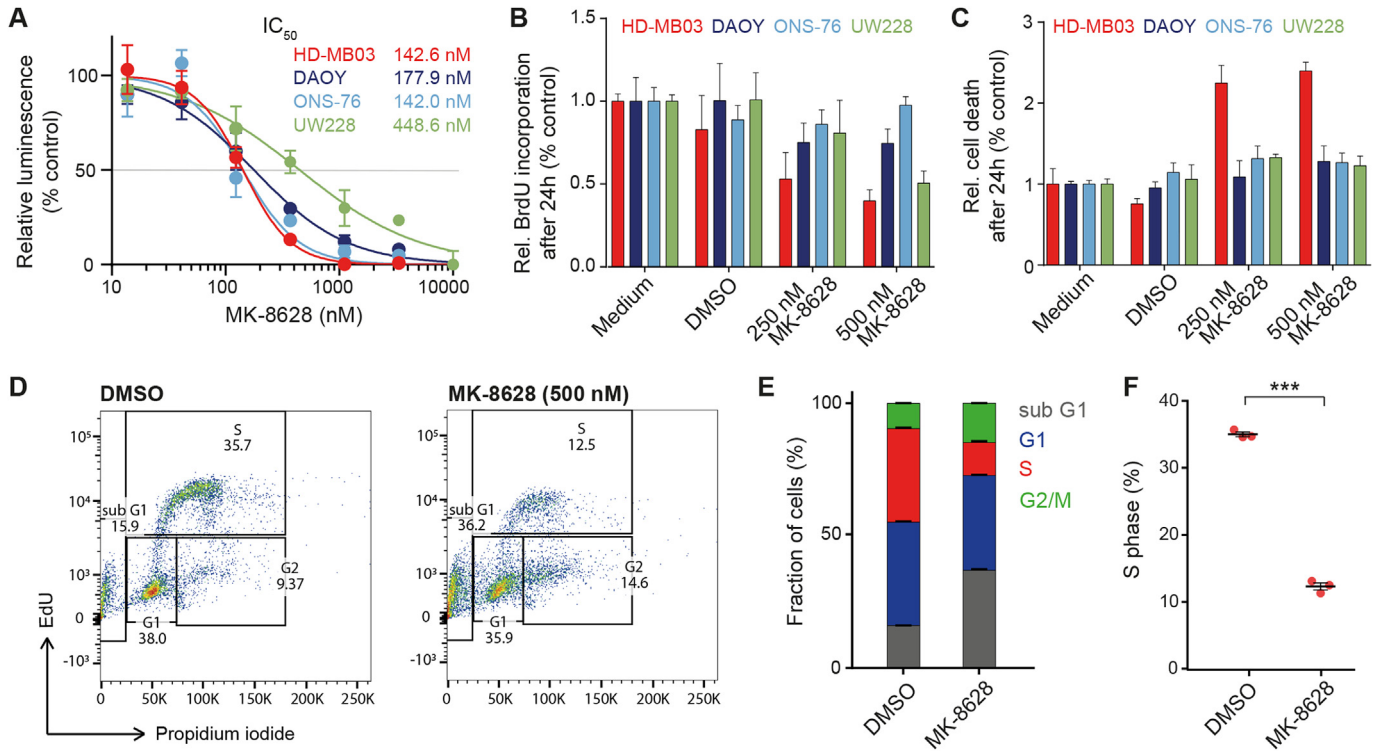

Fig. 1. MK-8628 exhibits significant anti-medulloblastoma effects *in vitro* at low nanomolar concentrations. (A) Dose response of four medulloblastoma cell lines treated with MK-8628 for 72h. Inhibitory concentrations of 50% viability (IC_{50}) are stated in the diagram. (Red: *MYC*-amplified; blue: non *MYC*-amplified with high MYC expression; green: non *MYC*-amplified with low MYC expression) **(B)** Relative BrdU incorporation of four medulloblastoma cell lines treated with MK-8628 (250 nM and 500 nM) or DMSO control for 24h. **(C)** Relative amount of cytoplasmic histone-associated DNA fragments, indicating cell death, in medulloblastoma cell lines treated with MK-8628 (250 nM, 500 nM) or DMSO control for 24h. **(D)** Cell cycle distribution of medulloblastoma cell line HD-MB03 after treatment with MK-8628 (500 nM) or DMSO control for 24h. **(E)** Fraction of HD-MB03 cells in each cell cycle phase after treatment with MK-8628 (500 nM) or DMSO control for 24h. **(F)** Fraction of HD-MB03 cells in S phase as measured in (E) (Student's t-test: * = $p < 0.05$, ** = $p < 0.01$, *** = $p < 0.001$).

2.5. Affymetrix microarrays, gene ontology and gene set enrichment analysis

HD-MB03 cells were plated at 1×10^5 cells/well in 6-well plates and after 12h were treated in triplicate with medium containing 0.2% DMSO (control) or 500 nM MK-8628-API for 24h. Total RNA was extracted using the RNeasyMini kit (Qiagen). Three replicates were treated and analyzed. Samples were profiled using the genechip Affymetrix Human Gene Expression Array (HG-U133 Plus 2.0, Affymetrix, Santa Clara, CA, USA) as described [37]. Microarray.CEL files were normalized and summarized to gene levels with RMA normalization [38]. Probes for which the log2 expression was ≥1.5 and had p-values ≤ 0.01 were considered as differentially expressed and picked for further analysis. Differential expression analysis was performed using limma package for R [39]. Hierarchical clustering was performed on the Euclidean distance of log2 expression values for the 50 most differentially expressed genes to visualize differential gene expression in HD-MB03 cells following MK-8628-API treatment. Gene ontology (GO) analysis and gene set enrichment (GSEA) analysis were performed using the clusterProfiler package in R [40]. The c6 oncogenic signatures (http://software.broadinstitute.org/gsea/msigdb/index.jsp) gene sets from Molecular Signatures Database (MSigDB) were used in this study. Furthermore we analyzed MYC signature scores (Dang [41], Kim [42], Schuhmacher [43], Westermann [44]). Agglomerative hierarchical clustering was performed using pairwise complete linkage and a Pearson correlation metric across both samples and genes.

2.6. Statistical analysis

Graph Pad Prism 7.0 (GraphPad Software Inc.) was used to calculate IC_{50} and the area under the curve (AUC) and to perform Kaplan-Meier survival analysis with log-rank statistics on treated and untreated mouse cohorts. Additionally, GraphPad was used to perform Student's two-sided t-tests to compare all interval variables, and the chi-square test was used for the comparison for all categorical variables. Fiji (NIH Image, Maryland, USA) was used for image analysis of western blot chemiluminescence images. Excess over Bliss was calculated using synergyfinder for R [45].

2.7. In vivo treatment of xenograft tumors in nude mice

HD-MB03 medulloblastoma cells were cultured to 80% confluency, harvested and suspended in 200 µL Matrigel™ (BD Bioscience, Heidelberg, Germany) for subcutaneous inoculation (1×10^7 cells per mouse, n = 24 mice) into the left flank of 4-week-old female athymic (nu/nu) mice. Mice were randomly assigned to either MK-8628-SD (Solid Dispersion) or vehicle control groups (n = 9 mice per group) after tumors reached 150–200 mm^3 in size. MK-8628-SD was administered using orogastric gavage. The mice were treated daily with water, 25 mg/kg MK-8628-SD, twice per day with 25 mg/kg MK-8628-SD or two times a week with cyclophosphamide 100 mg/kg. Tumor growth was monitored using a caliper and tumor volume was calculated using the formula (breadth × length × height)/2. Mice were euthanized by cervical dislocation when tumor size exceeded 2500 mm^3. To assess short term effects of MK-8628 treatment on molecular features of tumors, 6 doses of 50 mg/kg body weight MK-8628-SD or solvent (n = 3 mice each group) were administered at 0, 12, 24, 36, 48, 60 and 72h over a 3-day course. These mice were euthanized by cervical dislocation 4h after the last MK-8628-SD dose and xenograft tumors were excised from all mouse treatment cohorts, and divided into halves. Half the tissue was snap-frozen in liquid nitrogen then stored at −80 °C and the

other half was formalin-fixed and paraffin-embedded for further analysis. All animal experiments were performed in accordance with the Council of Europe guidelines for accommodation and care of laboratory animals, and protocols were approved by the Ethical Commission for Animal Experimentation at the University Hospital Essen.

3. Results

3.1. MK-8628 treatment reduces cell viability of medulloblastoma cell lines by inducing cell death and reducing cell proliferation

To test the anti-medulloblastoma activity of MK-8628, we treated four medulloblastoma cell lines with MK-8628 and measured relative ATP abundance over time. In all medulloblastoma cell lines treated with MK-8628 we observed a significant decrease in cell viability with increasing drug concentration (Fig. 1A, Suppl. Fig 1A, Suppl. Fig 1B). The concentration of MK-8628 leading to 50% growth inhibition (IC_{50}) were between 142.6 nM and 448.6 nM, similar to concentrations described for other BET inhibitors [17,37,46]. We observed that cell lines expressing higher *MYC* levels, HD-MB03, DAOY and ONS-76, showed lower IC_{50} values than UW228, which expresses low levels of *MYC* (Fig. 1A, Suppl. Fig 1A). Consistent with decreased cell viability, MK-8628 treatment led to a significant decrease in cell proliferation in medulloblastoma cells as evidenced by reduced BrdU incorporation after inhibitor treatment (Fig. 1B, Suppl. Fig 1C). Additionally, we observed that treatment with MK-8628 led to a significant increase in cell death in all cell lines, as measured by release of cytoplasmic histone-associated DNA fragments (Fig. 1C, Suppl. Fig 1D). To measure changes in cell cycle we performed EdU pulse labeling followed by fluorescence-activated cell sorting (FACS) measurement of the cell cycle distribution of HD-MB03 cells treated with MK-8628 (Fig. 1D). Consistent with the increase in cell death we observed an increase of the fraction of cells in sub G1 phase (Fig. 1E). Previous reports have shown that BET inhibition leads to cell cycle arrest in G1 and S phases due to BRD4's critical role in these processes [47,48]. Consistently, we observed a decrease in the fraction of cells in G1 and S phases (Fig. 1D, E and 1F). Taken together, treatment of medulloblastoma cell lines with MK-8628 leads to reduction in cell viability and cell proliferation and to increased cell death, to a similar extend as previously described for other BET inhibitors [16,17,37,46].

3.2. Pharmacological BRD4 inhibition with MK-8628 leads to repression of MYC expression and MYC-driven gene expression programs in medulloblastoma cell lines

BET inhibitors have been shown to lead to repression of *MYC* in medulloblastoma cells [13,17]. To assess the effect of BET inhibitor MK-8628 on *MYC* mRNA, MYC protein and MYC target gene expression we treated medulloblastoma cell lines with MK-8628 and performed qRT-PCR and western immunoblotting analysis of known BRD4-regulated targets [14]. MYC protein and mRNA expression was repressed after MK-8628 treatment, whereas CCND1 and WEE1 showed varying grades of repression (Fig. 2A, B, 2C and 2D, Suppl. Fig. 1E) [14,16,17]. BRD4 did not change in expression after MK-8628 treatment, consistent with disruption of its activity and not its expression (Fig. 2A, Suppl. Fig 1F). Even short term treatment with MK-8628 followed by treatment wash out led to reduction of *CCND1* expression for the following 24 h, suggesting that long-term target repression could be achieved with short-term inhibitor treatment (Fig. 2D). To assess the effect of MK-8628 on global gene expression programs *in vitro,* we performed gene expression microarray analysis of cells treated with MK-8628 compared to cells treated with DMSO control. A total of 6268 and 4982 genes were significantly up- or downregulated after MK-8628 treatment, respectively. Unsupervised clustering of the samples (3vs3) showed a clear separation of the top 50 differentially up- or downregulated genes according to the type of treatment (Fig. 2E). To assess the efficacy of MK-8628 to disrupt MYC-regulated transcriptional programs, we compared the observed gene expression changes with signatures calculated from published gene expression data of HD-MB03 treated with the BET inhibitor JQ1 [17] as well as from four published MYC/MYCN target gene signatures [41–44]. Consistent with similar pharmacological activity against BRD4, MK-8628 induced similar gene expression changes as previously reported for JQ1 treatment (Fig. 2F) [41–44]. As described for BRD4 inhibition, all four MYC/MYCN programs were significantly disrupted after MK-8628 treatment (Fig. 2F). Gene Ontology analysis (GO analysis) revealed that MK-8628 treatment lead to disruption of pathways related to chromatin regulation and neuronal development, consistent with previous reports on BRD4 functions in chromatin regulation and differentiation (Fig. 2G) [11,12]. A total of 45 pathways were significantly up- or downregulated after treatment with MK-8628 (Suppl. Table 1). Furthermore, gene set enrichment analysis (GSEA) showed a total of 50 pathways that were significantly up- or downregulated after treatment with MK-8628 (Suppl. Table 2). The significantly downregulated pathways included MYC pathway among others (Fig. 2H). Other pathways closely related to cancer development or to BET protein, such as E2F family, were also disrupted by MK-8628 treatment (Fig. 2H, Suppl. Table 2) [14]. In conclusion, MK-8628 treatment of MYC-driven medulloblastoma cells potently disrupts transcriptional programs regulated by BRD4.

3.3. Oral treatment with MK-8628 reduces tumor growth and induces apoptosis of human MYC-amplified group 3 medulloblastoma xenografts

Next, we assessed the efficacy of MK-8628 in an *in vivo* high-risk medulloblastoma model. We treated mice harboring xenografts of group 3 MYC-amplified HD-MB03 cells with MK-8628. In order to mimic clinically relevant conditions, oral treatment with MK-8628 was started when tumors where established and exponentially growing and had reached at least 200 mm^3 in volume. Oral MK-8628 treatment lead to a significant decrease in tumor growth over time (Fig. 3A). This decrease in tumor burden led to a significant survival advantage for mice treated with MK-8628 (Fig. 3B). However, treatment response was not curative and less effective than treatment with cyclophosphamide, a cytotoxic agent commonly used in medulloblastoma therapy, suggesting that monotherapy with BRD4 inhibitors may not have clinically relevant effects in patients with medulloblastoma (Fig. 3A and B). Interestingly, there was no significant difference in tumor growth between the mice treated once a day compared to mice treated twice daily (Fig. 3A and B). Consistent with our *in vitro* studies, we observed that the fraction of proliferating cells as measured by staining for Ki67 was significantly decreased in tumors treated with MK-8628 (Fig. 3C and D). Furthermore we observed a significant increase in apoptotic cells as measured by staining for cleaved caspase-3 in tumors from mice treated with MK-8628 (Fig. 3C and D). Together, MK-8628 significantly repressed cell proliferation and induced apoptosis *in vivo*, which led to reduced tumor growth over time and suggests that MK-8628 could have the potential to exhibit clinically relevant effects in patients suffering from medulloblastoma tumors.

3.4. Combination of BRD4 and PLK1 inhibitors have synergistic anti-MYC and anti-medulloblastoma effects in vitro

Even though treatment with MK-8628 showed promising anti-tumor activity *in vivo* (Fig. 3), these effects were not curative, which is in line with previous reports on BRD4 inhibitor *in vivo* activity [17]. We reasoned that combination of MK-8628 with other drugs affecting MYC expression might improve therapeutic effects. PLK1 inhibitors such as Volasertib and GSK461364A can potently reduce cell viability and suppress MYC protein expression in cancer cells [29–31]. Furthermore, in leukemia combined PLK1 and BRD4 inhibition has synergistic anti-leukemia effects [49]. We therefore hypothesized that combining MK-8628 with Volasertib or GSK461364A could also have synergistic

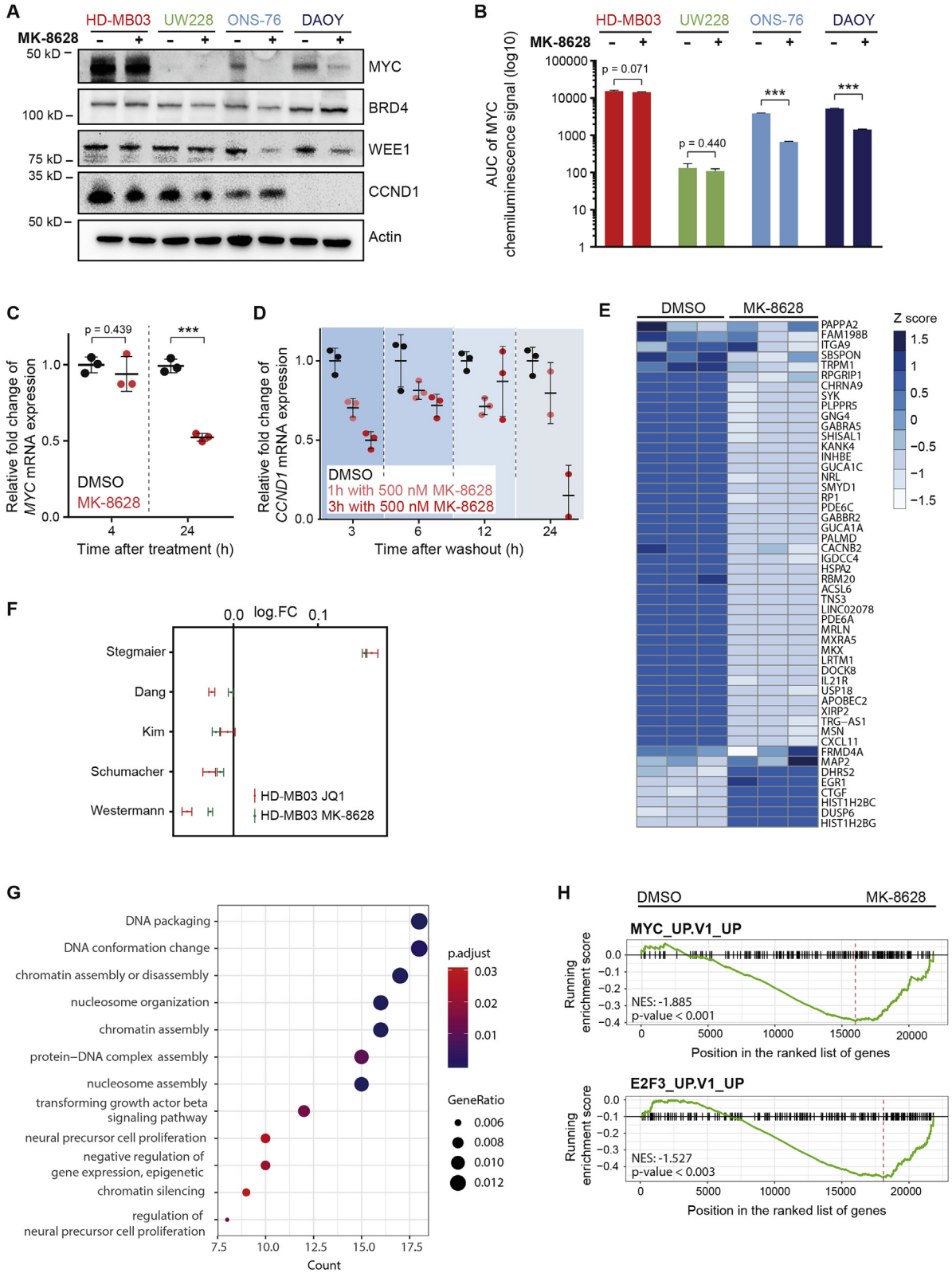

Fig. 2. MK-8628 treatment leads to repression of *MYC* transcription and protein expression. **(A)** Protein expression as measured using western immunoblotting of known BRD4 target genes compared after treatment of four medulloblastoma cell lines with MK-8628 (500 nM) or DMSO control for 24h. **(B)** Area under the curve (AUC) of the western immunoblotting chemiluminescence signals of MYC protein as measured in (A) (Student's t-test: * = $p < 0.05$, ** = $p < 0.01$, *** = $p < 0.001$). **(C)** *MYC* mRNA expression 4 and 24 h after MK-8628 treatment of medulloblastoma cell line HD-MB03 (Student's t-test: * = $p < 0.05$, ** = $p < 0.01$, *** = $p < 0.001$). **(D)** *CCND1* mRNA expression of medulloblastoma cell line HD-MB03 treated for 1 or 3 h with 500 nM MK-8628 or DMSO control, measured at 3, 6, 12 or 24 h after treatment washout. **(E)** Heatmap of the top 50 differentially expressed genes in HD-MB03 cells after treatment with MK-8628 compared to DMSO-treated cells. **(F)** Enrichment of the published *MYCN* gene expression signatures in differentially expressed genes after treatment with MK-8628 compared to JQ1-treated cells. **(G)** Gene ontology (GO) analysis of RNA expression changes in HD-MB03 cells treated with MK-8628 compared to DMSO control (x-axis = number of genes affected, size of circle indicating gene ration MK-8628 treatment vs. GO-term and circle color indicating adjusted p-value). **(H)** Two exemplary gene set enrichment analysis (GSEA) plots of the genes differentially expressed after treatment with MK-8628.

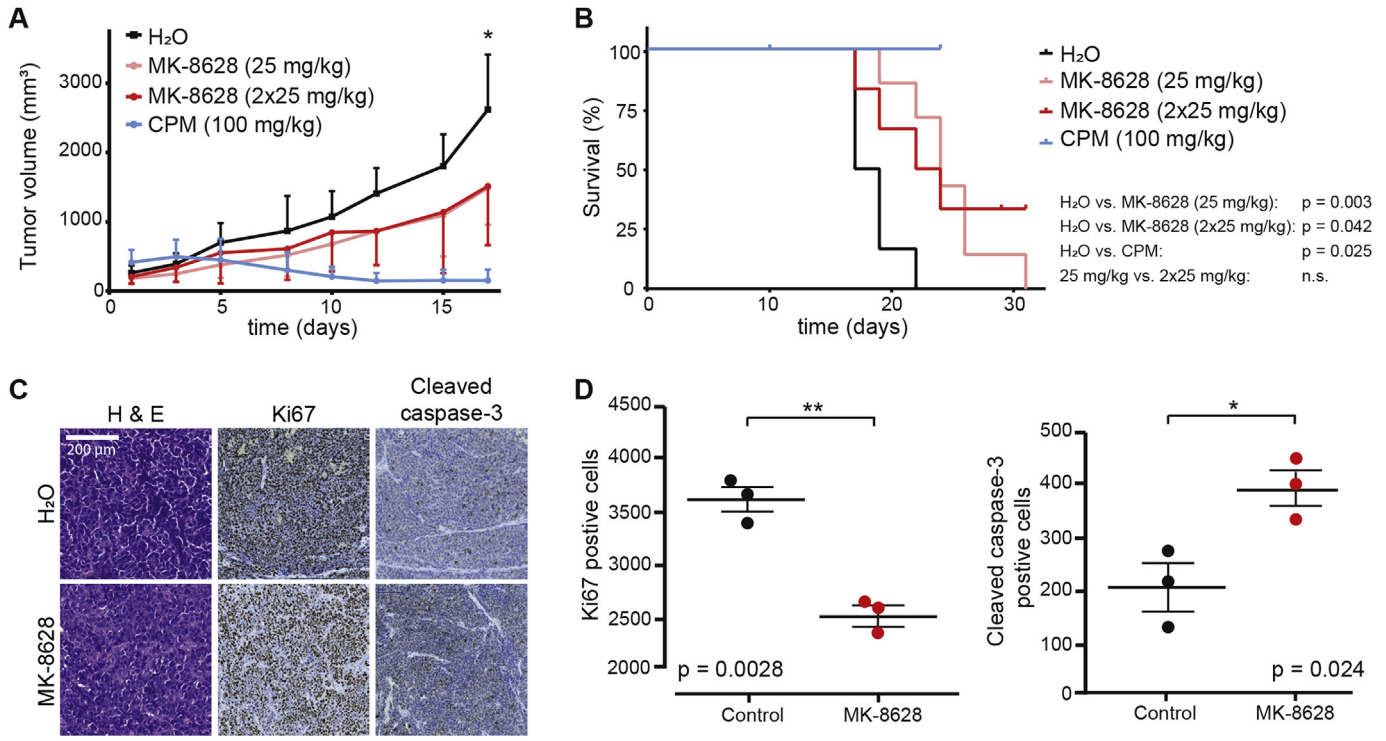

Fig. 3. MK-8628 treatment leads to decreased tumor growth and enhanced survival *in vivo*. **(A)** Tumor volume in nude mice harboring HD-MB03 xenografts treated with solvent (H_2O), cyclophosphamide (CPM) (100 mg/kg) or MK-8628 (25 or 2 × 25 mg/kg). **(B)** Kaplan Meier analysis of the overall survival of nude mice harboring HD-MB03 xenografts and treated with CPM (100 mg/kg) or MK-8628 (25 or 2 × 25 mg/kg) compared to mice treated with vehicle control (H_2O) (significance was calculated by log rank test). **(C)** Representative histological photomicrographs of tumors treated with MK-8628 or vehicle control (H & E: hematoxylin & eosin). **(D)** Quantitative analysis of photomicrographs of tumors treated with MK-8628 compared to tumors treated with vehicle control and stained for Ki67 (left) and cleaved caspase-3 (right) (Student's t-test: * = $p < 0.05$, ** = $p < 0.01$).

effects against medulloblastoma cells. To test this, we assessed the effect of Volasertib and GSK461364A on medulloblastoma cell viability. In all medulloblastoma cell lines treated with PLK1 inhibitors we observed a significant decrease in the number of viable cells with increasing inhibitor concentrations (Fig. 4A and Suppl. Fig. 2A). The IC_{50} ranged between 4.1 nM and 32.4 nM for Volasertib. Again, *MYC*-amplified HD-MB03 cells were most sensitive to Volasertib treatment, while UW228 cells, expressing low levels of *MYC*, were more resistant to treatment (Fig. 4A). The IC_{50} for GSK461364A ranged between 7.6 nM and 170.9 nM, except for DAOY cells which showed a high IC_{50} at 5285.0 nM (Suppl. Fig. 2A). Next, we assessed the synergistic effect of combined Volasertib and MK-8628 treatment on medulloblastoma cells. In HD-MB03, DAOY and ONS-76 cell lines, an excess over Bliss analysis indicated synergistic effects of combined PLK1 and BRD4 inhibitor treatment with highest synergy found at low drug concentrations, in particular in DAOY and ONS-76 cells (Fig. 4B, Suppl. Fig. 2B). Interestingly, combination treatment was antagonistic in UW228 cells, expressing low levels of *MYC*, suggesting that the efficacy of combined BRD4 and PLK1 inhibitor treatment might depend on *MYC* expression levels (Suppl. Fig. 2B). It was recently shown that Volasertib can bind to BRD4 [50,51]. In order to confirm that the synergy observed was independent of this activity, we tested combination treatment with MK-8628 and GSK461364A, a highly specific PLK1 inhibitor, in all four medulloblastoma cell lines. Again, combination treatment exhibited synergistic anti-medulloblastoma effects (Suppl. Fig. 2C). Consistent to these synergistic effect of MK-8628 combined with PLK1 inhibitors, addition of Volasertib to MK-8628 treatment led to a greater reduction of *MYC*, *CCND1* and *WEE1* expression compared to single agent treatment, which was accompanied by reduced PLK1 activity as evidenced by the reduction of PLK1 auto-phosphorylation (Fig. 4C and D). Synergistic effects on cell viability were accompanied with a significant increase in the fraction of apoptotic cells in sub G1 phase and a concomitant decrease in S phase, compared to single agent treatment (Fig. 4E, F and 4G and Suppl. Fig. 3). In summary, combined PLK1 and BRD4 inhibition exhibits synergistic anti-medulloblastoma effects which is accompanied by strong repression of BRD4 and PLK1 targets such as *MYC* mRNA expression and MYC protein stability (Fig. 4H).

4. Discussion

We here provide preclinical evidence for the therapeutic efficacy of BET bromodomain inhibitor MK-8628 in high-risk medulloblastoma. We show that single agent treatment with MK-8628, a small molecule BET bromodomain inhibitor, efficiently reduces cell viability and increases cell death for *in vitro* and *in vivo* models of high-risk medulloblastoma. These anti-tumor effects are accompanied by efficient transcriptional repression of *MYC* and its target genes as described for other BET inhibitors [16,17]. Additionally, we provide evidence that PLK1 inhibition can synergistically increase the anti-medulloblastoma effects of BRD4 inhibitors, providing a rationale for combined BRD4 and PLK1 inhibition in high-risk medulloblastoma.

In order to successfully introduce BRD4 inhibitors into clinical trials, adequate biomarkers for selection of patients, which are likely to respond, are clearly needed. While it has been challenging to identify markers predicting hypersensitivity to BET inhibitors, *MYC* and *MYCN* expression still remain the most commonly found features amongst responsive tumor cells [28]. Consistently, we and others have previously shown that *MYC*-expressing medulloblastoma cells are responsive to BET protein inhibition and that inhibition efficiently represses *MYC* transcription [16,17,21,22,52,53]. In line with previous findings, MK-8628 treatment also efficiently disrupted *MYC* transcription in *MYC*-amplified medulloblastoma which was further corroborated by our observation of highest induction of apoptosis by MK-8628 in cells harboring *MYC* amplifications. Tang et al. suggested that BRD4

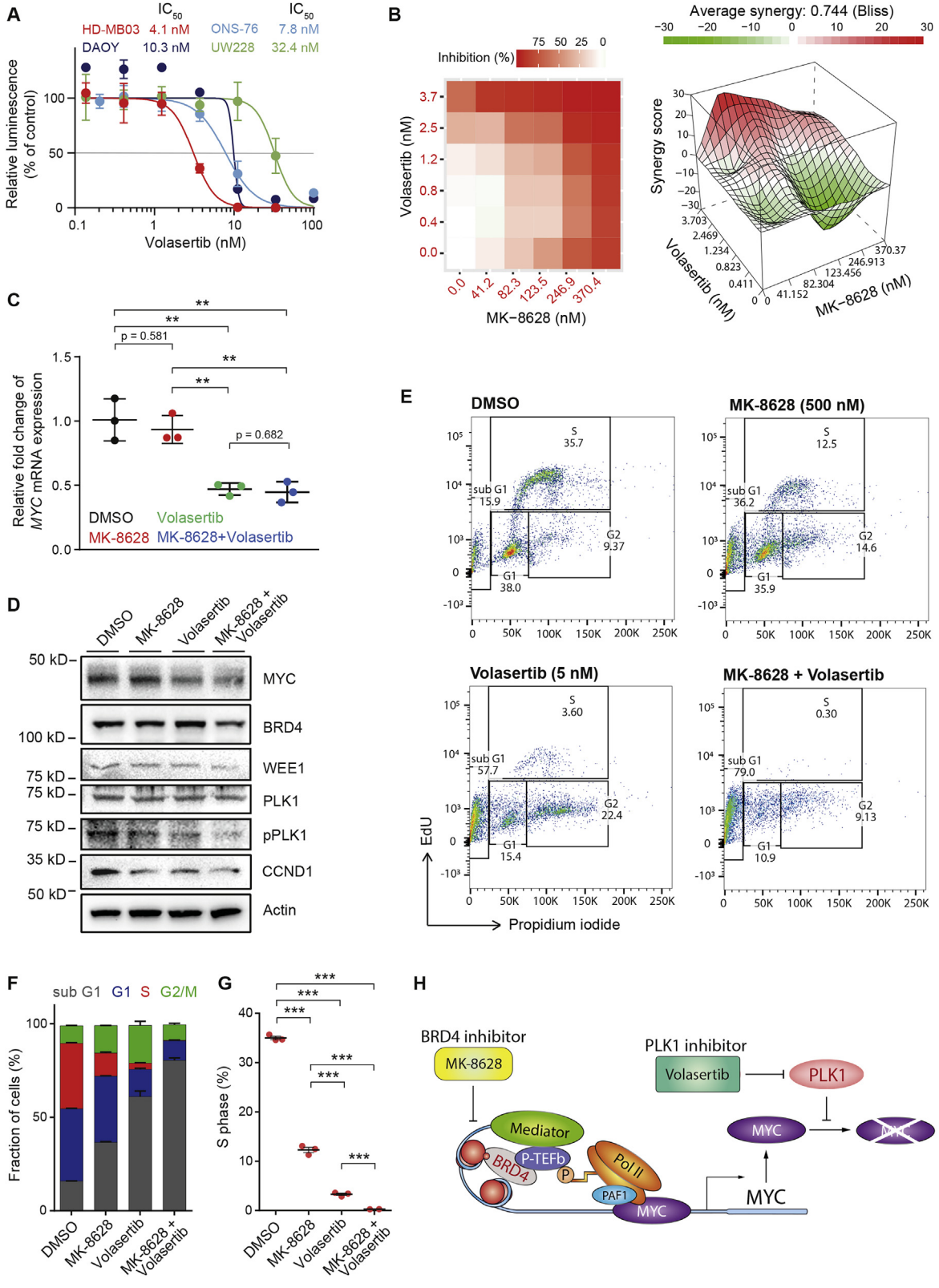

(caption on next page)

also regulates *GLI* transcription downstream of SMO in medulloblastoma from the SHH group [21]. Similar to Tang et al. we also observed considerable effects of MK-8628 in UW228 cells, which originate from a SHH medulloblastoma tumor and only expresses *MYC* at a low level. This raises the question, whether molecular features other than MYC may also predict susceptibility to BET inhibition. Some reports suggested that all genes regulated by enhancer regions marked with high H3K27 acetylation as well as high BRD4 occupancy (so called "super enhancers") are hypersensitive to BRD4 inhibition [53–56]. Consistently, both *MYC* and *GLI* are marked by such "super-enhancers" in group 3 and SHH medulloblastoma, respectively [53]. As both MYC status and SHH activation are clinically testable, these features might

Fig. 4. Combining BRD4 inhibitor MK-8628 and PLK1 inhibitor Volasertib has synergistic effects against high-risk medulloblastoma cells. (A) Dose response of four medulloblastoma cell lines treated with Volasertib for 72h. Inhibitory concentrations of 50% viability (IC_{50}) are stated in the diagram. **(B)** Excess over Bliss analysis of MYC-driven HD-MB03 cells treated with combinations of MK-8628 and Volasertib (red color indicates synergy). **(C)** Relative *MYC* mRNA expression as measured using qRT-PCR after treatment with MK-8628, Volasertib or combination treatment for 4h compared to vehicle control-treated cells (Student's t-test: * = $p < 0.05$, ** = $p < 0.01$). **(D)** Protein expression of BRD4 and PLK1 targets after treatment of medulloblastoma cell line HD-MB03 with DMSO control, MK-8628 (500 nM), Volasertib (5 nM), or combination of both (500 nM MK-8628 + 5 nM Volasertib) for 24h. **(E)** FACS-based measurement of the cell cycle distribution of HD-MB03 cells after treatment with DMSO control, MK-8628 (500 nM), Volasertib (5 nM), or combination of both (500 nM MK-8628 + 5 nM Volasertib) for 24h. **(F)** Fraction of HD-MB03 cells in each cell cycle phase after treatment with DMSO control, MK-8628 (500 nM), Volasertib (5 nM), or combination of both (500 nM MK-8628 + 5 nM Volasertib) for 24h. **(G)** Fraction of HD-MB03 cells in S phase as measured in (F) (Student's t-test: * = $p < 0.05$, ** = $p < 0.01$, *** = $p < 0.001$). **(H)** Schematic of the proposed mechanism of action of combined BRD4 and PLK1 inhibition in medulloblastoma based on previous models [34]. BRD4 is a regulator of gene transcription and inhibition of its binding to chromatin leads to repressed *MYC* mRNA expression. PLK1 is a kinase involved in regulation of protein degradation and its inhibition is known to lead to increased MYC protein degradation.

lend themselves as inclusion criteria for clinical trials with BET inhibitors. In order to advance BET inhibitors into clinical testing, however, further insight about biomarkers predicting susceptibility towards BET inhibition may be required.

Another prerequisite for successful clinical testing of targeted therapeutics is knowledge about pharmacodynamics markers that efficiently measure molecular response of tumors during treatment. Again, MYC protein and mRNA remains the most reliably observed molecular response marker in tumors treated with BRD4 inhibitors [17,37]. Why inhibition of BRD4, a global regulator of gene transcription, only leads to transcriptional repression of a subset of genes, most of them related to oncogenesis, is still under investigation [57]. Xu and Vakoc suggested that BRD4 inhibitors preferentially suppress genes that are dynamically expressed through exogenous stimuli or those expressed in a lineage-specific manner and thus are under influence of numerous trans- and cis-acting regulators [28]. Many growth and cancer promoting genes such as *MYC* are therefore suppressed after treatment with BET inhibitors in tumors and could be used as pharmacodynamics markers [28]. Consistently, *MYC* was also repressed after treatment of medulloblastoma cell lines with MK-8628 and therefore may be useful as a molecular marker for tumor response in future clinical trials.

Many BET inhibitors are currently being tested clinically, and it is still difficult to predict which drugs might have sufficient clinical potency and favorable pharmacological properties to be appropriate for clinical use. Comparison of gene expression changes induced by MK-8628 and JQ1 on medulloblastoma showed a high similarity of gene expression changes, indicating that MK-8628 and JQ1 are similarly specific BET inhibitors at nanomolar concentrations. In contrast to JQ1 and other BET inhibitors, MK-8628 is orally bioavailable, which might be advantageous for clinical use [24]. Similarly to other BET inhibitors, MK-8628 potently inhibited xenograft tumor growth, and significantly prolonged mouse survival in a MYC-driven xenograft model. The survival advantage observed in mouse xenograft models of high-risk medulloblastoma suggests that MK-8628 has the potential to generate a measurable response in this patient subgroup, which have dismal prognoses with current treatment regimens, and thus, should be a rationale for the clinical testing of MK-8628 in patients with medulloblastoma. However, MK-8628 as well as other inhibitors tested preclinically do not cure mice harboring medulloblastoma xenografts, suggesting that single-agent BRD4 inhibitor treatment might not have sufficient potency to cure patients suffering from medulloblastoma. Even patients suffering from a BRD4-driven disease such as NUT midline carcinoma, who initially respond well to BRD4 inhibitor-treatment, often relapse after several months [58]. This suggests that combination of BRD4 inhibitors with other therapeutics might be needed to efficiently treat patients suffering from medulloblastoma and other BRD4-dependent tumors.

There are many reports about combining BRD4 inhibitors with other targeted agents. For example drugs targeting PARP, HDAC, BCL2, mTOR and BRAF, respectively, have been shown to enhance anti-tumor efficacy of BRD4 inhibitors [59–65]. Many combinations show promising results in preclinical models; yet it will be challenging to select combinations for clinical trials, as most studies have been conducted in different tumor entities with different compounds and were assessed with different assays. One way to prioritize combination treatments may be to base their selection on our knowledge about their molecular mechanisms. As mentioned above, it is well described that BRD4 inhibition has significant effects on *MYC* expression and some, if not most, of its therapeutic effects, may be due to *MYC* repression. It is therefore likely that combining BRD4 inhibitors with other means of repressing *MYC* may potentiate the therapeutic effects of BRD4 inhibitors in a synergistic manner. Based on this idea, we selected to combine BRD4 and PLK1 inhibitors, as PLK1 inhibition is known to lead to increased MYC degradation [66]. This approach was recently shown to be successful in acute myeloid leukemia (AML) [33]. Consistent with reports in AML, combination of MK-8628 with Volasertib showed significant synergistic anti-medulloblastoma effects in *MYC*-expressing medulloblastoma cell lines but not cells expressing low levels of *MYC*. Interestingly, antagonistic effects were observed in UW228 cells, suggesting that other, yet to be defined mechanism of susceptibility to either BRD4 or PLK1 might be affected by inhibition of either target. This further substantiates the evidence that dual targeting of MYC by simultaneous inhibition of BRD4 and PLK1 might be a promising approach to increase therapeutic effects against a subset of medulloblastoma tumors. Intriguingly, several groups have recently described that many kinase inhibitors also have the ability to bind to the acetyllysine domain of BRD4, and Wang et al. explored and modulated the selectivity of such compounds and created selective dual inhibitors that target both PLK1 and BRD4 simultaneously [67]. Based on our observations about combining single-targeting BRD4 and PLK1 inhibitors, one might predict that the use of novel, dual-targeting agents might have the potential to generate clinically relevant therapeutic effects against MYC-driven tumors.

In summary, MK-8628 has promising preclinical anti-tumor activity against MYC-driven high-risk medulloblastoma, which can be potentiated by combination with PLK1 inhibitors. Further studies will be needed to carefully define *in vivo* activity of combination treatment once single agent phase I trials are completed and agents with favorable pharmacological properties are available, as this rationally devised strategy may have the potential to ameliorate the treatment of patients suffering from medulloblastoma.

Conflicts of interest

The authors have no conflict of interest to disclose.

Acknowledgements

A.G.H. is supported by the Deutsche Forschungsgemeinschaft – 398299703, the Berliner Krebsgesellschaft e.V., the Wilhelm Sander foundation and the Berlin Institute of Health. This work was supported by the German Cancer Foundation TransOnc program (ENABLE, 70112951). H.E.D. is supported by the Berlin Institute of Health (BIH) through TERMINATE-NB (CRG 04, 1.1.4.4). S.L. was supported by ASSET: Analysing and Striking the Sensitivities of Embryonal Tumours (FP7-HEALTH, ASSET).

Appendix A. Supplementary data

Supplementary data to this article can be found online at https://doi.org/10.1016/j.canlet.2018.12.012.

References

[1] M.D. Taylor, P.A. Northcott, A. Korshunov, M. Remke, Y.-J. Cho, S.C. Clifford, et al., Molecular subgroups of medulloblastoma: the current consensus, Acta Neuropathol. 123 (4) (2012) 465–472.

[2] P.A. Northcott, A.M. Dubuc, S. Pfister, M.D. Taylor, Molecular subgroups of medulloblastoma, Expert Rev. Neurother. 12 (7) (2012) 871–884.

[3] V. Ramaswamy, M. Remke, E. Bouffet, S. Bailey, S.C. Clifford, F. Doz, et al., Risk stratification of childhood medulloblastoma in the molecular era: the current consensus, Acta Neuropathol. 131 (6) (2016) 821–831.

[4] D.W. Ellison, M. Kocak, J. Dalton, H. Megahed, M.E. Lusher, S.L. Ryan, et al., Definition of disease-risk stratification groups in childhood medulloblastoma using combined clinical, pathologic, and molecular variables, J. Clin. Oncol. 29 (11) (2011) 1400–1407.

[5] M. Kool, A. Korshunov, M. Remke, D.T. Jones, M. Schlanstein, P.A. Northcott, et al., Molecular subgroups of medulloblastoma: an international meta-analysis of transcriptome, genetic aberrations, and clinical data of WNT, SHH, Group 3, and Group 4 medulloblastomas, Acta Neuropathol. 123 (4) (2012) 473–484.

[6] Y.J. Cho, A. Tsherniak, P. Tamayo, S. Santagata, A. Ligon, H. Greulich, et al., Integrative genomic analysis of medulloblastoma identifies a molecular subgroup that drives poor clinical outcome, J. Clin. Oncol. 29 (11) (2011) 1424–1430.

[7] S. Hacker, S. Karl, I. Mader, S. Cristofanon, T. Schweitzer, J. Krauss, et al., Histone deacetylase inhibitors prime medulloblastoma cells for chemotherapy-induced apoptosis by enhancing p53-dependent Bax activation, Oncogene 30 (19) (2011) 2275–2281.

[8] B. Barneda-Zahonero, M. Parra, Histone deacetylases and cancer, Mol. Oncol. 6 (6) (2012) 579–589.

[9] D. Horiuchi, B. Anderton, A. Goga, Taking on challenging targets: making MYC druggable, Am. Soc. Clin. Oncol. Edu. Book (2014) e497–502.

[10] P. Filippakopoulos, J. Qi, S. Picaud, Y. Shen, W.B. Smith, O. Fedorov, et al., Selective inhibition of BET bromodomains, Nature 468 (7327) (2010) 1067–1073.

[11] S.Y. Wu, C.M. Chiang, The double bromodomain-containing chromatin adaptor Brd4 and transcriptional regulation, J. Biol. Chem. 282 (18) (2007) 13141–13145.

[12] S. Rahman, M.E. Sowa, M. Ottinger, J.A. Smith, Y. Shi, J.W. Harper, et al., The Brd4 extraterminal domain confers transcription activation independent of pTEFb by recruiting multiple proteins, including NSD3, Mol. Cell Biol. 31 (13) (2011) 2641–2652.

[13] J.E. Delmore, G.C. Issa, M.E. Lemieux, P.B. Rahl, J. Shi, H.M. Jacobs, et al., BET bromodomain inhibition as a therapeutic strategy to target c-Myc, Cell 146 (6) (2011) 904–917.

[14] A. Puissant, S.M. Frumm, G. Alexe, C.F. Bassil, J. Qi, Y.H. Chanthery, et al., Targeting MYCN in neuroblastoma by BET bromodomain inhibition, Cancer Discov. 3 (3) (2013) 308–323.

[15] H. Herrmann, K. Blatt, J. Shi, K.V. Gleixner, S. Cerny-Reiterer, L. Mullauer, et al., Small-molecule inhibition of BRD4 as a new potent approach to eliminate leukemic stem- and progenitor cells in acute myeloid leukemia AML, Oncotarget 3 (12) (2012) 1588–1599.

[16] P. Bandopadhayay, G. Bergthold, B. Nguyen, S. Schubert, S. Gholamin, Y. Tang, et al., BET bromodomain inhibition of MYC-amplified medulloblastoma, Clin. Canc. Res. 20 (4) (2014) 912–925.

[17] A. Henssen, T. Thor, A. Odersky, L. Heukamp, N. El-Hindy, A. Beckers, et al., BET bromodomain protein inhibition is a therapeutic option for medulloblastoma, Oncotarget 4 (11) (2013) 2045–2056.

[18] J.E. Bolden, N. Tasdemir, L.E. Dow, J.H. van Es, J.E. Wilkinson, Z. Zhao, et al., Inducible in vivo silencing of Brd4 identifies potential toxicities of sustained BET protein inhibition, Cell Rep. 8 (6) (2014) 1919–1929.

[19] K. Althoff, A. Beckers, E. Bell, M. Nortmeyer, T. Thor, A. Sprussel, et al., A Cre-conditional MYCN-driven neuroblastoma mouse model as an improved tool for preclinical studies, Oncogene 34 (26) (2014 Jun) 3357–3368, https://doi.org/10.1038/onc.2014.269 Epub 2014 Sep 1.

[20] A.G. Henssen, K. Althoff, A. Odersky, A. Beckers, R. Koche, F. Speleman, et al., Targeting MYCN-driven transcription by BET-bromodomain inhibition, Clin. Canc. Res. 22 (10) (2015 May 15) 2470–2481, https://doi.org/10.1158/1078-0432.CCR-15-1449 Epub 2015 Dec 2.

[21] Y. Tang, S. Gholamin, S. Schubert, M.I. Willardson, A. Lee, P. Bandopadhayay, et al., Epigenetic targeting of Hedgehog pathway transcriptional output through BET bromodomain inhibition, Nat. Med. 20 (7) (2014) 732–740.

[22] S. Venkataraman, I. Alimova, I. Balakrishnan, P. Harris, D.K. Birks, A. Griesinger, et al., Inhibition of BRD4 attenuates tumor cell self-renewal and suppresses stem cell signaling in MYC driven medulloblastoma, Oncotarget 5 (9) (2014) 2355–2371.

[23] J.K.I.K. Noel, S. Ooike, K. Sugahara, H. Nakamura, M. Daibata, Development of the BET bromodomain inhibitor OTX015, Proceeding of the 2013 AACR- NCI-EORTC Molecular Targets and Cancer Therapeutics Conference, 2013, p. 414.

[24] M. Boi, E. Gaudio, P. Bonetti, I. Kwee, E. Bernasconi, C. Tarantelli, et al., The BET bromodomain inhibitor OTX015 affects pathogenetic pathways in preclinical B-cell tumor models and synergizes with targeted drugs, Clin. Canc. Res. 21 (7) (2015) 1628–1638.

[25] M.M. Coude, T. Braun, J. Berrou, M. Dupont, S. Bertrand, A. Masse, et al., BET inhibitor OTX015 targets BRD2 and BRD4 and decreases c-MYC in acute leukemia cells, Oncotarget 6 (19) (2015) 17698–17712.

[26] P. Herait, C. Berthon, C. Thieblemont, E. Raffoux, V. Magarotto, A. Stathis, et al., BET-bromodomain inhibitor OTX015 shows clinically meaningful activity at non-toxic doses: interim results of an ongoing phase I trial in hematologic malignancies, in: Research IPottAMotAAfC (Ed.), AACR; 2014 Apr 5-9; San Diego, CA. Philadelphia (PA), 2014.

[27] A phase I pharmacokinetic study of OTX015 for the treatment of patients with hematologic malignancies, in: E. Odore, K. Rezai, E. Riveiro, F. Bourdel, P. Herait, E. Cvitkovic, et al. (Eds.), Proceedings of the 105th Annual Meeting of the American Association for Cancer Research; 2014 Apr 5-9, Cancer Research, San Diego, 2014.

[28] Y. Xu, C.R. Vakoc, Targeting cancer cells with BET bromodomain inhibitors, Cold Spring Harb. Perspect. Med. 7 (7) (2017).

[29] S. Ackermann, F. Goeser, J.H. Schulte, A. Schramm, V. Ehemann, B. Hero, et al., Polo-like kinase 1 is a therapeutic target in high-risk neuroblastoma, Clin. Canc. Res.:Offic. J. Am. Assoc. Canc. Res. 17 (4) (2011) 731–741.

[30] Z. Liu, Q. Sun, X. Wang, PLK1, A potential target for cancer therapy, Translat. Oncol. 10 (1) (2016) 22–32.

[31] J. Triscott, C. Lee, C. Foster, B. Manoranjan, M.R. Pambid, R. Berns, et al., Personalizing the treatment of pediatric medulloblastoma: Polo-like kinase 1 as a molecular target in high-risk children, Cancer Res. 73 (22) (2013) 6734–6744.

[32] J. Tan, Z. Li, P.L. Lee, P. Guan, M.Y. Aau, S.T. Lee, et al., PDK1 signaling toward PLK1-MYC activation confers oncogenic transformation, tumor-initiating cell activation, and resistance to mTOR-targeted therapy, Cancer Discov. 3 (10) (2013) 1156–1171.

[33] U. Tontsch-Grunt, D. Rudolph, I. Waizenegger, A. Baum, D. Gerlach, H. Engelhardt, et al., Synergistic activity of BET inhibitor BI 894999 with PLK inhibitor volasertib in AML in vitro and in vivo, Cancer Lett. 421 (2018) 112–120.

[34] R.L. Yauch, Dijkgraaf GJP, B. Alicke, T. Januario, C.P. Ahn, T. Holcomb, et al., Smoothened mutation confers resistance to a hedgehog pathway inhibitor in medulloblastoma, Science 326 (5952) (2009) 572–574.

[35] A.G. Henssen, C. Reed, E. Jiang, H.D. Garcia, J. von Stebut, I.C. MacArthur, et al., Therapeutic targeting of PGBD5-induced DNA repair dependency in pediatric solid tumors, Sci. Transl. Med. 9 (414) (2017).

[36] J. Vandesompele, K. De Preter, F. Pattyn, B. Poppe, N. Van Roy, A. De Paepe, et al., Accurate normalization of real-time quantitative RT-PCR data by geometric averaging of multiple internal control genes, Genome Biol. 3 (7) (2002) RESEARCH0034.

[37] A. Henssen, K. Althoff, A. Odersky, A. Beckers, R. Koche, F. Speleman, et al., Targeting MYCN-driven transcription by BET-bromodomain inhibition, Clin. Canc. Res.: Offic. J. Am. Assoc. Canc. Res. 22 (10) (2016) 2470–2481.

[38] R.C. Gentleman, V.J. Carey, D.M. Bates, B. Bolstad, M. Dettling, S. Dudoit, et al., Bioconductor: open software development for computational biology and bioinformatics, Genome Biol. 5 (10) (2004) R80.

[39] F. Hong, R. Breitling, C.W. McEntee, B.S. Wittner, J.L. Nemhauser, J. Chory, RankProd: a bioconductor package for detecting differentially expressed genes in meta-analysis, Bioinformatics 22 (22) (2006) 2825–2827.

[40] G. Yu, L.G. Wang, Y. Han, Q.Y. He, clusterProfiler: an R package for comparing biological themes among gene clusters, OMICS 16 (5) (2012) 284–287.

[41] K.I. Zeller, A.G. Jegga, B.J. Aronow, K.A. O'Donnell, C.V. Dang, An integrated database of genes responsive to the Myc oncogenic transcription factor: identification of direct genomic targets, Genome Biol. 4 (10) (2003) R69.

[42] Y.H. Kim, L. Girard, C.P. Giacomini, P. Wang, T. Hernandez-Boussard, R. Tibshirani, et al., Combined microarray analysis of small cell lung cancer reveals altered apoptotic balance and distinct expression signatures of MYC family gene amplification, Oncogene 25 (1) (2006) 130–138.

[43] M. Schuhmacher, F. Kohlhuber, M. Holzel, C. Kaiser, H. Burtscher, M. Jarsch, et al., The transcriptional program of a human B cell line in response to Myc, Nucleic Acids Res. 29 (2) (2001) 397–406.

[44] F. Westermann, D. Muth, A. Benner, T. Bauer, K.O. Henrich, A. Oberthuer, et al., Distinct transcriptional MYCN/c-MYC activities are associated with spontaneous regression or malignant progression in neuroblastomas, Genome Biol. 9 (10) (2008) R150.

[45] L. He, E. Kulesskiy, J. Saarela, L. Turunen, K. Wennerberg, T. Aittokallio, et al., Methods for high-throughput drug combination screening and synergy scoring, Methods Mol. Biol. 1711 (2018) 351–398.

[46] M.-M. Coudé, T. Braun, J. Berrou, M. Dupont, S. Bertrand, A. Masse, et al., BET inhibitor OTX015 targets BRD2 and BRD4 and decreases c-MYC in acute leukemia cells, Oncotarget 6 (19) (2015) 17698–17712.

[47] V. Sahai, A.J. Redig, K.A. Collier, F.D. Eckerdt, H.G. Munshi, Targeting BET bromodomain proteins in solid tumors, Oncotarget 7 (33) (2016) 53997–54009.

[48] Z. Yang, N. He, Q. Zhou, Brd4 recruits P-TEFb to chromosomes at late mitosis to promote G1 gene expression and cell cycle progression, Mol. Cell Biol. 28 (3) (2008) 967–976.

[49] S. Abbou, C. Lanvers-Kaminsky, E. Daudigeos-Dubus, L. LE Dret, C. Laplace-Builhe, J. Molenaar, et al., Polo-like kinase inhibitor volasertib exhibits antitumor activity and synergy with Vincristine in pediatric malignancies, Anticancer Res. 36 (2) (2016) 599–609.

[50] P. Ciceri, S. Muller, A. O'Mahony, O. Fedorov, P. Filippakopoulos, J.P. Hunt, et al., Dual kinase-bromodomain inhibitors for rationally designed polypharmacology, Nat. Chem. Biol. 10 (4) (2014) 305–312.

[51] D. Rudolph, M.A. Impagnatiello, C. Blaukopf, C. Sommer, D.W. Gerlich, M. Roth, et al., Efficacy and mechanism of action of volasertib, a potent and selective inhibitor of Polo-like kinases, in preclinical models of acute myeloid leukemia, J. Pharmacol. Exp. Therapeut. 352 (3) (2015) 579–589.

[52] B. Knoechel, J.E. Roderick, K.E. Williamson, J. Zhu, J.G. Lohr, M.J. Cotton, et al., An epigenetic mechanism of resistance to targeted therapy in T cell acute

lymphoblastic leukemia, Nat. Genet. 46 (4) (2014) 364–370.
[53] J. Loven, H.A. Hoke, C.Y. Lin, A. Lau, D.A. Orlando, C.R. Vakoc, et al., Selective inhibition of tumor oncogenes by disruption of super-enhancers, Cell 153 (2) (2013) 320–334.
[54] B. Chapuy, M.R. McKeown, C.Y. Lin, S. Monti, M.G. Roemer, J. Qi, et al., Discovery and characterization of super-enhancer-associated dependencies in diffuse large B cell lymphoma, Cancer Cell 24 (6) (2013) 777–790.
[55] W.A. Whyte, D.A. Orlando, D. Hnisz, B.J. Abraham, C.Y. Lin, M.H. Kagey, et al., Master transcription factors and mediator establish super-enhancers at key cell identity genes, Cell 153 (2) (2013) 307–319.
[56] M. Muhar, A. Ebert, T. Neumann, C. Umkehrer, J. Jude, C. Wieshofer, et al., SLAM-seq defines direct gene-regulatory functions of the BRD4-MYC axis, Science 360 (6390) (2018) 800–805.
[57] M. Perez-Salvia, M. Esteller, Bromodomain inhibitors and cancer therapy: from structures to applications, Epigenetics 12 (5) (2017) 323–339.
[58] A. Stathis, E. Zucca, M. Bekradda, C. Gomez-Roca, J.P. Delord, T. de La Motte Rouge, et al., Clinical response of carcinomas harboring the BRD4-NUT oncoprotein to the targeted bromodomain inhibitor OTX015/MK-8628, Cancer Discov. 6 (5) (2016) 492–500.
[59] P.K. Mazur, A. Herner, S.S. Mello, M. Wirth, S. Hausmann, F.J. Sanchez-Rivera, et al., Combined inhibition of BET family proteins and histone deacetylases as a potential epigenetics-based therapy for pancreatic ductal adenocarcinoma, Nat. Med. 21 (10) (2015) 1163–1171.
[60] L. Paoluzzi, D. Hanniford, E. Sokolova, I. Osman, F. Darvishian, J. Wang, et al., BET and BRAF inhibitors act synergistically against BRAF-mutant melanoma, Cancer Med. 5 (6) (2016) 1183–1193.
[61] R. Vazquez, M.E. Riveiro, L. Astorgues-Xerri, E. Odore, K. Rezai, E. Erba, et al., The bromodomain inhibitor OTX015 (MK-8628) exerts anti-tumor activity in triple-negative breast cancer models as single agent and in combination with everolimus, Oncotarget 8 (5) (2017) 7598–7613.
[62] L. Yang, Y. Zhang, W. Shan, Z. Hu, J. Yuan, J. Pi, et al., Repression of BET activity sensitizes homologous recombination-proficient cancers to PARP inhibition, Sci. Transl. Med. 9 (400) (2017).
[63] L.T. Lam, X. Lin, E.J. Faivre, Z. Yang, X. Huang, D.M. Wilcox, et al., Vulnerability of small-cell lung cancer to apoptosis induced by the combination of BET bromodomain proteins and BCL2 inhibitors, Mol. Canc. Therapeut. 16 (8) (2017) 1511–1520.
[64] J.C. Enssle, C. Boedicker, M. Wanior, M. Vogler, S. Knapp, S. Fulda, Co-targeting of BET proteins and HDACs as a novel approach to trigger apoptosis in rhabdomyosarcoma cells, Cancer Lett. 428 (2018) 160–172.
[65] S. Karakashev, H. Zhu, Y. Yokoyama, B. Zhao, N. Fatkhutdinov, A.V. Kossenkov, et al., BET bromodomain inhibition synergizes with PARP inhibitor in epithelial ovarian cancer, Cell Rep. 21 (12) (2017) 3398–3405.
[66] D. Xiao, M. Yue, H. Su, P. Ren, J. Jiang, F. Li, et al., Polo-like kinase-1 regulates myc stabilization and activates a feedforward circuit promoting tumor cell survival, Mol. Cell 64 (3) (2016) 493–506.
[67] J. Wang, T. Erazo, F.M. Ferguson, D.L. Buckley, N. Gomez, P. Muñoz-Guardiola, et al., Structural and atropisomeric factors governing the selectivity of pyrimido-benzodiazipinones as inhibitors of kinases and bromodomains, ACS Chem. Biol. 13 (9) (2018 Sep 21) 2438–2448, https://doi.org/10.1021/acschembio.7b00638 Epub 2018 Aug 31.